JOURNAL OF MATERIALS SCIENCE 23 (1988) 2595–2600

EXAFS study of polymorphs of manganese dioxides

JIAN-BAO LI, KUNIHITO KOUMOTO, HIROAKI YANAGIDA
Department of Industrial Chemistry, Faculty of Engineering, University of Tokyo, 7-3-1 Hongo, Bunkyo-ku, Tokyo 113, Japan

An attempt has been made to use extended X-ray absorption fine structure (EXAFS) to study the polymorphs (beta, gamma and alpha types, and ramsdellite) of manganese dioxides. The ratio of (1 × 1) tunnels to (1 × 2) tunnels for the intergrowth structure of gamma-MnO_2 was found to be as high as 46.2%. The relation between the valence state of manganese ions and the threshold absorption energy (E_0) was clarified and E_0 was found to be in the following order: beta > gamma > alpha (K) > alpha (Ba). EXAFS presented a possibility of nondestructive analysis of the valence state of manganese ions in manganese dioxides.

1. Introduction

The phenomenon of extended X-ray absorption fine structure (EXAFS) refers to the oscillatory modulation of the X-ray absorption coefficient as a function of X-ray photon energy beyond the absorption edge. The existence of such an extended fine structure was known and treated theoretically in the 1930s by Kronig [1–3], and was recently developed by Stern and co-workers [4, 5]. This technique has been gradually established as a practical structural tool to be used for amorphous solids, liquid, solutions, catalysts and surface science. But little is so far known concerning the attempts of EXAFS study in ceramic science because ceramic materials are normally used in dense crystalline forms. In practice, however, EXAFS has an outstanding nature in that the information about a given guest atom species of interest can be selectively isolated from host materials, so that this technique is expected to be applied widely to the study of structure and properties of ceramic materials.

We have studied the relations between valence states, crystal structure and material properties for manganese oxide systems [6, 7]. Manganese is an element which has various valence states showing +7, +4, +3, +2 and 0 valences. The difference in the valence states in the oxides causes the positions and nature of the chemical bond of cations in the crystal structure to differ from one another and eventually produces profound effects on the material properties. In this paper, an attempt was made to use a laboratory EXAFS system to study the polymorphs of manganese oxides and to perform EXAFS measurements for crystalline ceramics. The application limitations for EXAFS as a study tool of the intergrowth structure of polymorphs are discussed.

2. Experimental details

2.1. Preparation of materials [8]

The dioxide polymorphs beta-MnO_2, gamma-MnO_2, potassium-bearing alpha-MnO_2 (cryptomelane) and barium-bearing alpha-MnO_2 (hollandite) were employed for EXAFS measurements. High purity (99.9%) beta-MnO_2, purchased from Rare Metallic Co., Ltd, Japan, was chosen as the model compound because it has a basic MnO_2 structure and its composition is very close to stoichiometry compared to other polymorphs of manganese dioxides. For gamma-MnO_2 the International Common Samples No. 15 of manganese dioxides (International Battery Society, IBS) was used. Alpha-MnO_2 was prepared by the chemical reaction between $KMnO_4$ and $MnCl_2$ in sulphuric acid solution at 90° C [10]. The resultant product, $K_{2-x}Mn_8O_{16}$, forms a cryptomelane structure. Barium-bearing alpha-MnO_2 was derived from the Gawari Wadhona Mine, India ($Ba_{0.77}K_{0.19}Mn_8O_{16}$) and was supplied by Miura and Hariya [11]. These compounds were further crushed, and powdered to a sufficiently fine size.

2.2. Apparatus and measurement conditions

The EXAFS apparatus used for the measurement is installed at the High Power X-ray Centre of the Engineering Research Institute (University of Tokyo, Japan) [12]. The system demonstrated in Fig. 1 consists of a high power rotating-anode X-ray generator (RU-1000) as an X-ray source, optical components (a Soller slit, a monochromator and other slits), a solid state detector (SSD), counting circuitry and a microcomputer. In the measurement Ge (1 1 1), a channel-cut and flat crystal monochromator was used, and the high power rotating-anode X-ray generator was operated typically at a tube voltage of 30 kV and a tube current of 500 mA. Under these conditions the data collection time was normally 30 h for almost all of the manganese compounds. The central hole of the holder in a thin film which was 0.01 to 0.03 mm in depth was filled with powders of these compounds which had been ground to a sufficiently fine size; it was then fixed between the two cellophane adhesive tapes on both sides. Special care was needed to achieve uniformity of the sample. Measurements were made in air at room temperature.

0022–2461/88 $03.00 + .12

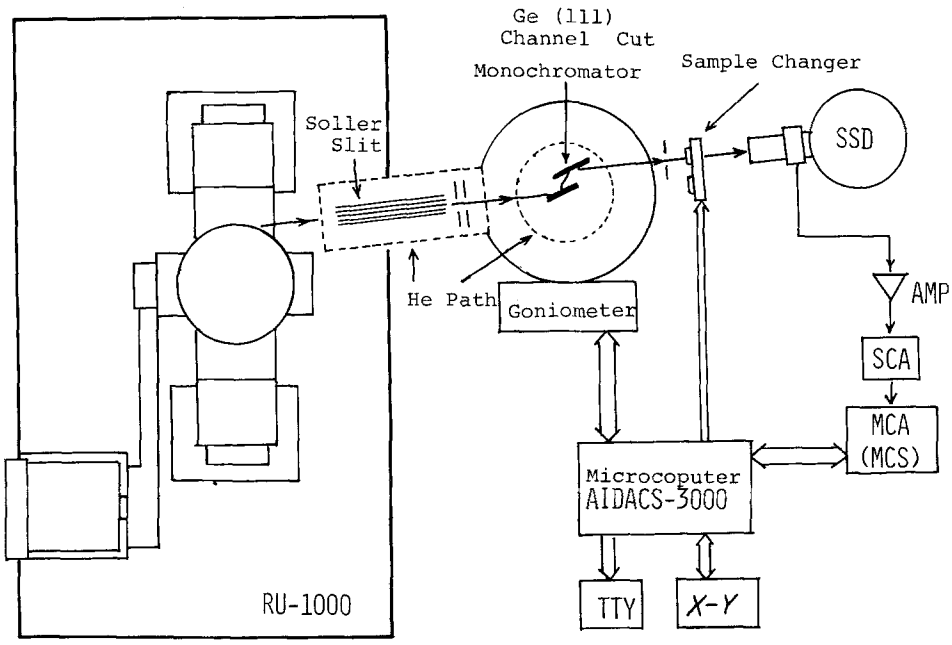

Figure 1 Schematic drawing of the EXAFS apparatus.

3. Data analysis and results

Data analyses were done in the computer centre of the University of Tokyo using the computer program written by the Kuroda laboratory (Department of Chemistry, Faculty of Science, University of Tokyo, Japan). This analysis procedure is shown as a flow chart in Fig. 2. These EXAFS spectra were obtained by the measurement of the absorption coefficient, μ or μt, as a function of X-ray photon energy (see Fig. 3, where t is the sample thickness). From the absorption spectrum the oscillation is isolated by appropriate datum reduction.

The first step in the analysis is to isolate $X(K)$ from the total absorption coefficient data $\mu(E)$. The background was removed by the "cubic spline" routine [13]. After converting the EXAFS spectrum from the

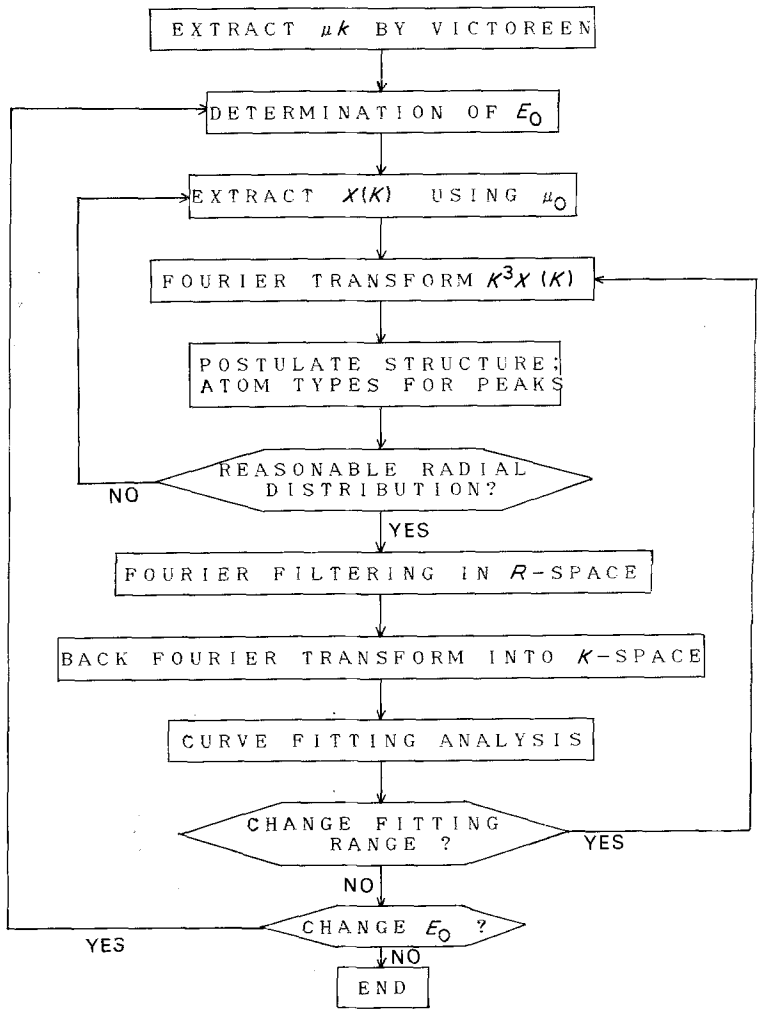

Figure 2 Flow chart of analysis for EXAFS spectroscopy.

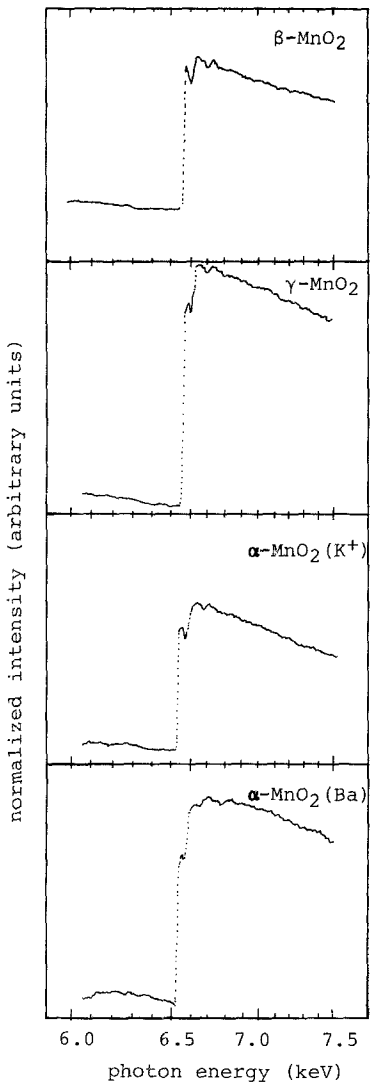

Figure 3 K-edge EXAFS spectra of manganese dioxides.

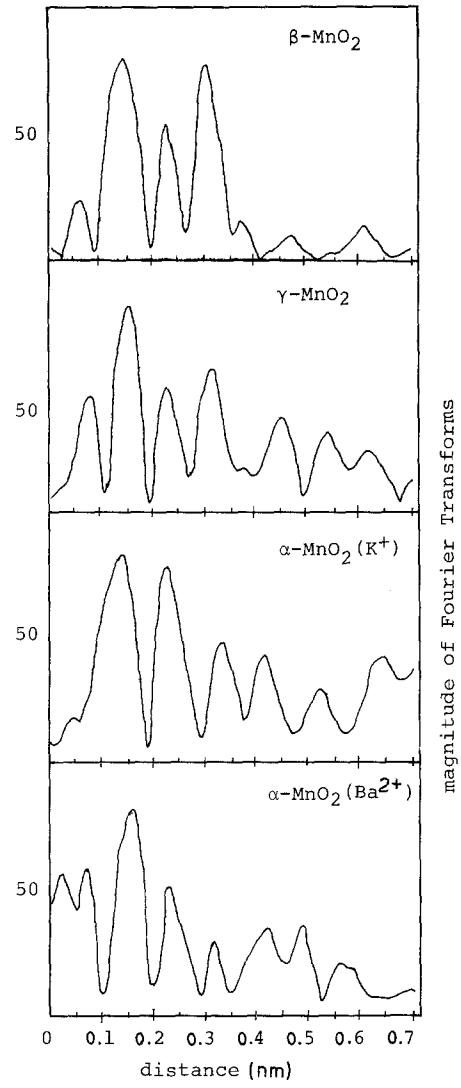

Figure 4 Fourier transform magnitudes, $K^3 X(K)$, of manganese dioxides.

experimental values of photon energy, $\hbar\omega$, to the k-space and removing the smooth background using a spline fit and multiplying by k^3, the $k^3 X(k)$ obtained is Fourier transformed from the k-space to the R (distance)-space to yield a function similar to a radial distribution. The obtained $|F(r)|$ for the samples are plotted in Fig. 4. The components at the low values of $R(R < 0.1\,\text{nm})$ are due to any remaining smooth absorption background, and those of $R > 0.4\,\text{nm}$ are mainly due to the random statistical counting noise. The peaks between $0.1\,\text{nm} < R < 0.4\,\text{nm}$ were analysed. The Fourier transform at these values of R ($0.1\,\text{nm} < R < 0.4\,\text{nm}$) provides a first guess for the true structure. To obtain the distance it is necessary to Fourier transform the $F(r)$ back to the k-space over a limited range of R (for the major peaks) by inverse Fourier transformation, called Fourier filtering or curve-filtering analysis. Fig. 5 shows an example of Fourier filtered data (solid lines) of the major peaks in Fig. 4. The dashed curves show attempted fits to the filtered data. After removing the background, multiplying by k^3, Fourier filtering, separating the amplitude and phase, and curve fitting, the parameters R (interatomic distance) of these samples were calculated and are shown in Table I. The two results from the EXAFS data and X-ray diffraction data show excellent agreement.

The threshold absorption energies of the manganese ions in the polymorphs are shown in Table II. For the sake of comparison, the measurement conditions and parameters for computation were chosen in a similar manner.

TABLE I Interatomic distances obtained by EXAFS analysis

Sample	EXAFS data			X-ray, R (nm)
	Neighbour atom	R (nm)	$r^\dagger$	
β-MnO_2*	Mn–O	0.1880	0.180	0.188
	Mn–Mn	0.287	0.142	0.287
	Mn–Mn	0.406	0.039	0.406
γ-MnO_2	Mn–O	0.1894	0.166	0.189
	Mn–Mn	0.2833	0.047	0.287
	Mn–Mn	0.4082	0.042	
α-MnO_2 (K)	Mn–O	0.1845	0.356	0.189
	Mn–Mn	0.2858	0.084	0.285
	Mn–Mn	0.4230	0.071	
α-MnO_2 (Ba)	Mn–O	0.1895	0.018	0.189
	Mn–Mn	0.2833	0.118	0.285
	Mn–Mn	0.4061	0.068	

*Corrected values.
† Debye factor.

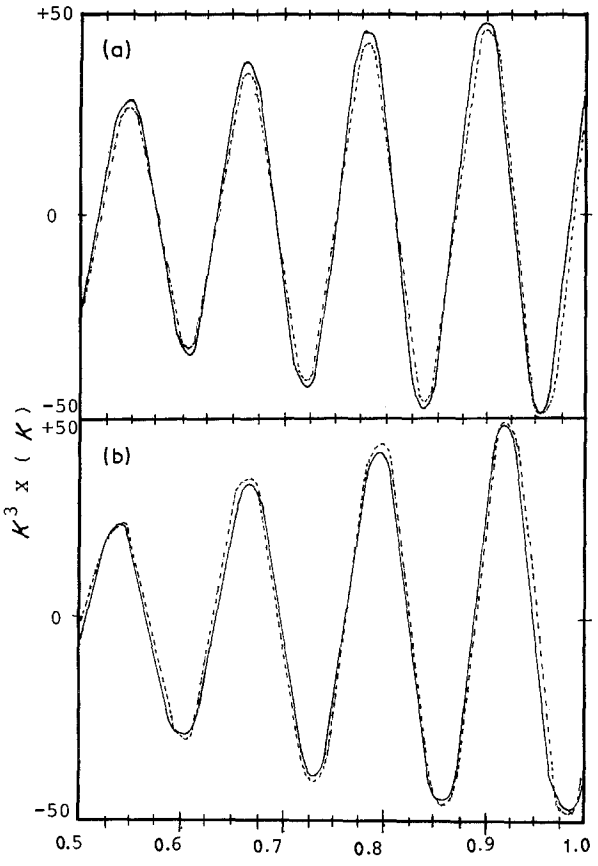

Figure 5 Two of the curve fitting data for the peak between 0.26 and 0.30 nm. (——) Observed, (– – –) calculated curves. (a) Barium-bearing alpha MnO_2 (r = 0.296 nm). (b) Potassium-bearing alpha MnO_2 (r = 0.284 nm).

4. Discussion

4.1. Structures of polymorphs of manganese dioxide

The MnO_2 polymorphs bear, collectively, a tunnel structure as a common structure unit which is formed by edge sharing or corner sharing of (MnO_6) octahedra [14]. The polymorphs are distinguished from each other by the tunnel sizes that are defined by the product of the numbers of (MnO_6) octahedra on the abscissa and on the ordinate (number of ordinate × number of abscissa as (1 × 1), (1 × 2)) in the cross-section. Beta-MnO_2, which has a relatively stoichiometric composition and isostructure with rutile (TiO_2), consists almost of (1 × 1) tunnels, and ramsdellite consists of only (1 × 2) tunnels. The width of the two species of tunnels are similarly in one dimension and these phases easily form domain intergrowth. Another common polymorph, gamma-MnO_2, which is used as an oxidizing agent for dry-cells, consist of irregular random intergrowth of the (1 × 1) tunnel units and (1 × 2) tunnel units (Fig. 6). Such tunnel structures and their intergrowths have recently become noted, because difference in the tunnel size may affect unique material characteristics such as electrical conductivity [7], the discharge of dry cell [15], ion-exchange [16] ion-absorption [17], gas reactivity [18], etc. It is clearly important to identify the tunnel sizes in order to elucidate the existence of the intergrowth of these tunnel structures and to calculate the fraction of each tunnel unit. To data, there has been no technique, which directly measures the intergrowth structure of the polymorphs [19]. The present study is an attempt of such, made by means of EXAFS spectroscopy.

TABLE II Absorption edge energy (keV) for manganese oxides

Sample	E_0 (eV)
β-MnO_2	6561.48
γ-MnO_2	6542.59
α-MnO_2 (K)	6538.82
α-MnO_2 (Ba)	6531.31

4.2. The relation between the coordination number and the ratio of intergrowths

In Fig. 5, three large peaks in the distance range 0.1 to 0.36 nm can be seen for all the manganese dioxides. On comparing the peaks of the polymorphs, it is seen that the heights of these peaks are different; both the height and position shift of peaks particularly in the range 0.3 to 0.36 nm becoming lower in the order beta > gamma > alpha (K) > alpha (Ba). The position and the height of the peaks correspond to the distance and the coordination number, respectively. The results of analysis of these peaks, shown in Table I, agree with the X-ray diffraction data.

The coordination number, which can be applied to estimate the polymorph structure is etimated from the peaks in the distance range 0.341 to 0.354 nm. As shown in Fig. 6b, the coordination number is eight for beta-MnO_2 with (1 × 1) tunnels only and four for ramsdellite with 1 × 2 tunnels. Gamma-MnO_2 has a coordination number between four and eight due to the intergrowth of (1 × 1) tunnels and (1 × 2) tunnels. The coordination number shows a change from four to eight depending on the ratio of the two tunnels in the structure caused by the difference in the preparation conditions and annealing temperature [7]. The more (1 × 1) tunnels in gamma-MnO_2 structure exist, the larger the coordination number becomes. So the coordination number at a distance 0.341 to 0.354 nm can be used to estimate the ratio of (1 × 1) tunnels and (1 × 2) tunnels intergrowing in gamma-MnO_2. Table III shows the coordination number of the gamma-MnO_2 of the International Common Sample. The number, Nr, corrected by the model compound is as high as 5.752. Using the formula $[(Nr - 4)/4] \times 100\%$, the percentage of (1 × 1) tunnels in the gamma-MnO_2 of IC15 is 43.8% and others (56.2%) are (1 × 2) tunnels. That is a reasonable value for a material of common dry cells [7, 15].

TABLE III Observed (Nr') and corrected (Nr). Coordination numbers of Mn–Mn at a distance R the percentage of (1 × 1) tunnels ($P_{1\times1}$) in gamma-MnO_2, and the Debye factor, d_{E_0}

	β-MnO_2	γ-MnO_2
R (nm)	0.3449	0.3448
Nr'	1.655	1.119
Nr	8.0	5.752
$P_{1\times1}$	100%	43.80%
d_{E_0}	0.039	0.042

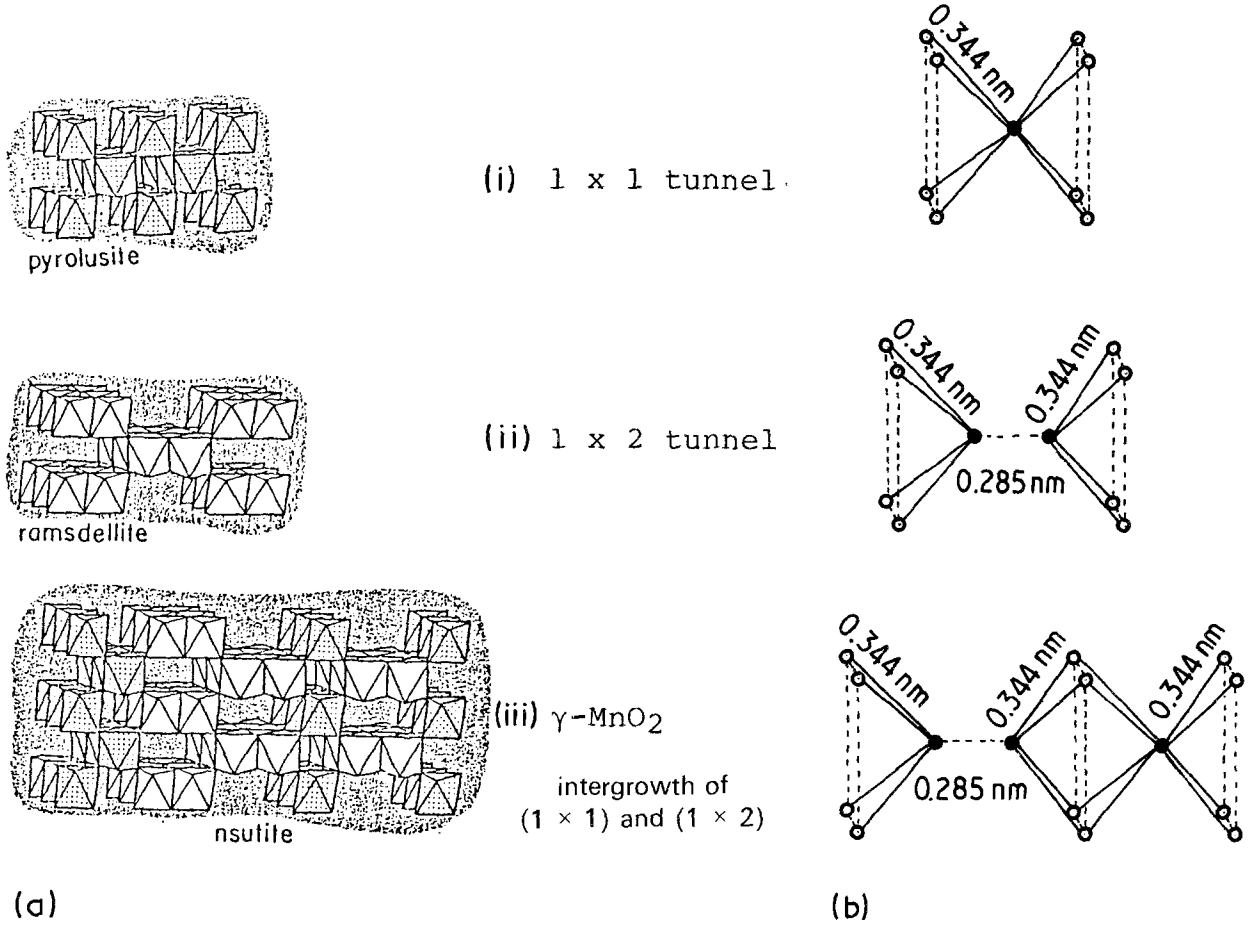

Figure 6 (a) structure of manganese dioxides. (i) Pyrolusite containing (1 × 1) tunnels; (ii) ramsdellite containing (1 × 2) tunnels; (iii) gamma-MnO_2 containing a random intergrowth of (1 × 1) and (1 × 2) tunnels. (b) Schematic illustration of coordination numbers of Mn–Mn with a distance of 0.344 nm.

4.3. Relation between E_0 and the valence state

Although the manganese ions in the polymorphs mentioned above are almost tetravalent, trivalent manganese ions Mn^{3+} exist to a certain extent, and their concentrations in the polymorphs are different from each other. Beta-MnO_2 is a stoichiometric compound in which most of the manganese ions are tetravalent, while gamma-MnO_2 contains a certain amount of trivalent ions, Mn^{3+}, due to its non-stoichiometric composition, $MnO_{1.75}$–$MnO_{19.5}$. Alpha-MnO_2 contains lower valence guest cations in the tunnel structure and so has more trivalent ions than the gamma-type due to charge compensation. Hollandite doped with divalent ions, Ba^{2+}, has more Mn^{3+} than cryptomelane doped with monovalent ions, K^+. Thus the concentration of trivalent ions, Mn^{3+}, tends to increase in the order beta < gamma < alpha (K) < alpha (Ba). It is of importance to obtain correctly the concentration of trivalent ions, Mn^{3+}, for the study of relations between valence, structure and property. However, the analysis of the valence is so far considered to be difficult because valence-disproportionation (for example; $Mn^{4+} + Mn^{2+} = 2\,Mn^{3+}$) occurs easily when using water as a solvent in the usual chemical analysis method. The threshold absorption energy, E_0, measurement by EXAFS would give us an alternate method for valence analysis.

The threshold absorption energy, E_0, of manganese ions was found in 6500 eV region of photon energy. In Fig. 5, the position (E_0) of the first peak shifts gradually from the high energy to the low energy region in the order beta-type > gamma-type > alpha-type. Table II shows the E_0 values calculated from the peaks. This order coincides with the order of increase in the concentration of trivalent ions Mn^{3+}, and hence the deviation from stoichiometry. Because the E_0 shift of EXAFS corresponds to the valence state of manganese ions, it can be used to estimate the average valence of manganese ions in an unknown sample.

5. Conclusions

As shown in Table III, the ratio of (1 × 1) tunnels to (1 × 2) tunnels intergrown in the polymorph gamma-MnO_2 structure was calculated from the coordination number by the EXAFS data. As shown in Table II, the relation between E_0 and the valence of manganese ions in the polymorphs was found and this would make possible a nondestructive comparison of valences of manganese ions in the polymorphs. Although it was confirmed that EXAFS can be applied to study polymorphs of manganese dioxide, the present study is a first attempt and still incomplete from a quantitative viewpoint. Further investigation of EXAFS application to ceramic materials including metallic oxides, is desired.

Acknowledgements

The authors gratefully acknowledge the experimental help of Mr Kazuo Ono, and thank Mr Tomoaki Tanase for the data analysis and his technical assistance in the measurements. They also thank Mr Hiroyuki Iwasaki for his assistance with computer operation and also the members of Kuroda laboratory, University of Tokyo, for giving the authors an opportunity to use their EXAFS analysis program.

References

1. R. D. L. KRONIG, *Z. Phys.* **70** (1931) 317.
2. *Idem, ibid.*, **75** (1932) 191.
3. *Idem, ibid.* **75** (1932) 468.
4. E. A. STERN, *Phys. Rev. B.* **10** (1974) 3027.
5. D. E. SAYERS, F. W. LYTLE and E. A. STERN, *Adv. X-ray Anal.* **13** (1970) 248.
6. J. B. LI, K. KOUMOTO, H. YANAGIDA, 25th Symposium of Basic Science of Ceramics, Okaka, Japan, 1D15 (1986).
7. J. B. LI, K. KOUMOTO, H. YANAGIDA, *J. Ceram. Soc. Jpn* **96** (1988) 74.
8. J. B. LI, K. KOUMOTO and H. YANAGIDA, Proceeding of the Annual Meeting, *Ceram. Soc. Jpn Nagoya* **3A22** (1987) 741.
9. A. KOZAWA, *J. Electrochem. Soc.* **119** (1972) 152C.
10. M. TSUJI and M. ABE, *Solv. Extr. Ion. Exchange* **5** (1984) 253.
11. H. MIURA and Y. HARIYA, Proceeding of the Annual Meeting, *Mineral. Soc. Jpn Tokyo* **B-5** (1985) 49.
12. Y. SATO, PhD thesis, University of Tokyo, (1982).
13. S. P. CRAMER, K. O. HODGSON, E. I. STIEFEL and N. E. NEWTON, *J. Amer. Chem. Soc.* **100** (1978) 2748.
14. R. BURNS, Battery Material Symposium, Vol. 1, Brussels (1983) pp. 342–4.
15. J. P. BRENET, 3rd MnO_2 Symposium, Graz (1985) pp. 16–18.
16. A. D. WADSLEY, *J. Amer. Chem. Soc.* **72** (1950) 1981.
17. C. BIGLIOCCA, F. GIRAIDI, J. PAULY and E. SABBIONI, *Analy. Chem.* **39** (1967) 1634.
18. J. B. LI, K. KOUMOTO and H. YANAGIDA, *J. Mater. Sci. Lett.* (1988) 331.
19. S. TURNER and P. R. BUSECK, *Science* **212** (1981) 1024.

Received 22 August
and accepted 1 December 1987